

## Echo-planar magnetic resonance imaging studies of frontal cortex activation during word generation in humans

(echo-planar imaging/gradient-echo/deoxyhemoglobin/magnetic susceptibility)

GREGORY MCCARTHY<sup>†‡§</sup>, ANDREW M. BLAMIRE<sup>¶</sup>, DOUGLAS L. ROTHMAN<sup>||</sup>, ROLF GRUETTER<sup>¶</sup>,  
AND ROBERT G. SHULMAN<sup>¶</sup>

Departments of <sup>†</sup>Surgery (Neurosurgery), <sup>¶</sup>Molecular Biophysics and Biochemistry, and <sup>||</sup>Internal Medicine, Yale University School of Medicine, New Haven, CT 06510; and <sup>‡</sup>Neuropsychology Laboratory 116B1, Veteran's Administration Medical Center, West Haven, CT 06516

Contributed by Robert G. Shulman, February 17, 1993

**ABSTRACT** Nine subjects were studied by high-speed magnetic resonance imaging while performing language-based tasks. Subjects were asked either to repeat or to generate verbs associated with nouns read by an experimenter while magnetic resonance images were obtained of the left inferior frontal lobe. The echo-planar imaging sequence was used with a gradient echo time of 70 ms to give an apparent transverse relaxation time weighting ( $T_2^*$ ) that is sensitive to local hemoglobin levels. Images were acquired every 3 s (repetition time) in series of 32. In plane resolution was  $6 \times 4.5$  mm and slice thickness was 10 mm. An increase in signal accompanied performance of the tasks, with significantly more activation for verb generation than for repeating. The activation effect occurred within 3 s after task onset and could be observed in single images from individual subjects. The primary focus of activation appeared in gray matter along a sulcus anterior to the lateral sulcus that included the anterior insula, Brodmann's area 47, and extending to area 10. Little or no activation of this region was found for a passive listening, covert generation, or mouth-movement control tasks. Significant activation was also found for a homologous region in the right frontal cortex but not for control regions in calcarine cortex. These results are consistent with prior studies that have used positron emission tomography imaging with  $^{15}\text{O}$ -labeled water as a blood flow tracer.

New techniques for studying the human brain *in vivo* have excited interest in its functional anatomy. Techniques such as positron emission tomography (PET), which measures the distribution of radioactive tracers within the brain, have provided strong evidence for localized brain activation during functional tasks. Petersen and colleagues (1–3) used PET with  $^{15}\text{O}$ -labeled water as a blood flow tracer to identify brain regions associated with the sensory processing of words, with the motor and articulatory aspects of speech production, and with the generation of “uses” for given nouns. The latter task primarily involved left inferior frontal cortex (LIFC) including Brodmann's area 47, suggesting a role for this region in semantic processing (3). Frith and colleagues (4) have shown left frontal activation during verbal fluency tasks, although the primary region of activation was more dorsal, near Brodmann's area 46.

Magnetic resonance imaging (MRI) methods for localizing dynamic brain processes have recently been developed (5, 6). One of these techniques exploits differences in the magnetic susceptibility of oxygenated and deoxygenated hemoglobin to track blood-flow-related phenomena with high temporal and spatial resolution (6–11). The effect is observed in difference images between task and control conditions, so that it is advantageous to use fast imaging methods to reduce

flow and movement artifacts. These methods show effects in single images in individual subjects, in contrast to most PET studies, which rely upon group averages.

Fast MRI has been used successfully to demonstrate activation by sensory stimulation and motor tasks (5–11). In this report, we used echo-planar imaging (EPI; ref. 12) to study the time course and localization of brain activation during word-processing tasks. The tasks and brain regions were selected to allow direct comparison with recent PET studies (1–3).

### METHODS

**Subjects.** Nine right-handed subjects (three female) were studied. Two subjects moved their heads significantly during tasks and their data were therefore discarded. The study was approved by the Human Investigation Committee of Yale University and each subject gave informed consent. Subjects were placed supine on the patient bed of a modified 2.1-T Biospec 1 spectrometer (Bruker ORS, Billerica, MA) equipped with Oxford Magnet Technologies (Oxford) shielded gradients. Each subject wore ear plugs throughout the study that were connected with sound tubes to a mouthpiece worn by an experimenter for communication. A second sound tube was used to monitor the subject's spoken responses during the tasks. The subject's head was firmly secured in a foam rubber holder to reduce movement during the experiment and was then positioned inside a birdcage RF coil (13).

**MRI.** To localize the plane of study in the frontal cortex, four sagittal, multislice,  $T_1$ -weighted images [inversion time ( $T_{IR}$ ) = 810.0 ms, echo time ( $TE$ ) = 17.4 ms, repetition time ( $T_R$ ) = 2.1s] were acquired. The line between the anterior and posterior commissures (AC–PC line) was identified and projected into the frontal lobe. An axial slice of 10-mm thickness was centered 8 mm below the AC–PC line in the frontal lobe to encompass the region activated in the PET studies (1–3). The inferior frontal lobe has a very inhomogeneous magnetic field caused by the sinuses. To maximize the task-related signal changes, the magnetic field within the left or right frontal lobe was made more homogeneous by using an automated routine that simultaneously adjusted all first- and second-order shim currents (14). The shimmed region generally included Brodmann's areas 47, 10, and 22. Total set up time was  $\approx 1.5$  hr.

Functional images were acquired using a spin-echo version of the EPI sequence (10) with an apparent transverse relaxation time ( $T_2^*$ ) weighting of 70 ms between the spin-echo and

The publication costs of this article were defrayed in part by page charge payment. This article must therefore be hereby marked “advertisement” in accordance with 18 U.S.C. §1734 solely to indicate this fact.

Abbreviations: EPI, echo-planar imaging; LIFC, left inferior frontal cortex; MRI, magnetic resonance imaging; PET, positron emission tomography; ROI, region of interest;  $T_2$ , transverse relaxation time;  $T_2^*$ , apparent transverse relaxation time; Hb, deoxyhemoglobin;  $T_R$ , repetition time;  $TE$ , echo time;  $T_{IR}$ , inversion time.

<sup>§</sup>To whom reprint requests should be addressed.

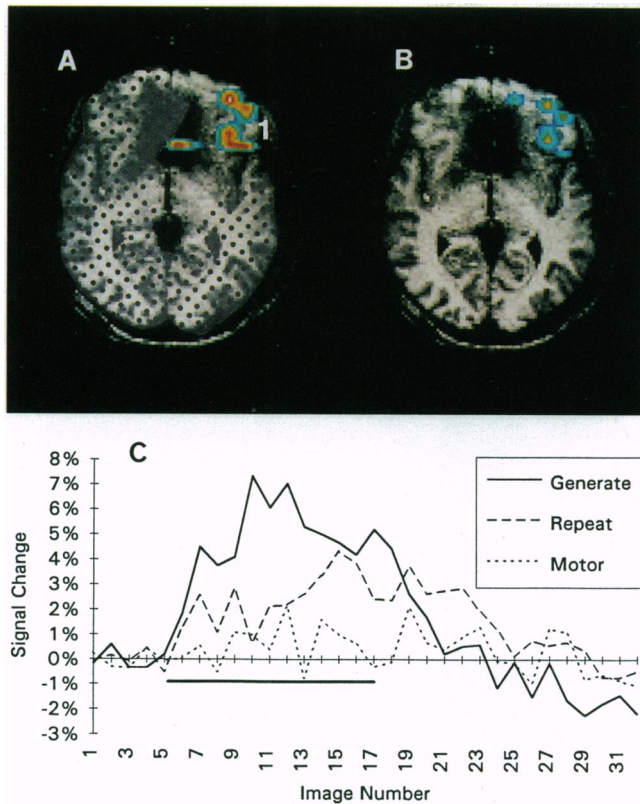


FIG. 1. (A) The color overlays represent z-score deviations of the first Generate condition from the first Baseline condition (see text). In this and all subsequent figures, increasing z-score values are represented by warmer colors. z scores with associated probabilities below 0.05 are not represented. The overlays are superimposed upon a  $T_1$ -weighted image acquired during the same imaging session. The dots represent regions from which little signal was obtained following shimming optimized for the LIFC. The ROI marked as "1" includes areas 47 and 10. (B) The color overlays represent a direct comparison of the Generate and Repeat conditions. (C) Time course of the activation effect measured as  $\Delta S/S_0$  for Generate, Repeat, and Motor measured for ROI 1 of A. The horizontal bar below the abscissa represents the active task period beginning after image 5 and ending at image 17.

the center of the acquisition to give susceptibility related contrast. The image matrix size was  $64 \times 64$  with nominal in-plane resolution of  $6 \times 4.5$  mm and slice thickness of 10 mm. A  $T_R$  of 3 s was used between successive images to reduce saturation effects.

**Tasks.** Subjects were engaged in four core conditions that were repeated in random order two or three times per session. Thirty-two images were acquired of the selected plane in each condition for a total time of 96 s. In *Baseline*, subjects rested for the entire 32-image set with no stimuli. In *Motor*, subjects rested during images 1–5 (pre-task), moved their tongue and lips or jaws (but refrained from speech and subvocalizing) during images 6–17 (active task), and rested during images 18–32 (post-task). The remaining tasks followed the same protocol, with the active task always performed during images 6–17. In *Repeat*, subjects were read a list of common nouns (approximately 1 word per 1.5 s) and asked to repeat each word immediately. In *Generate*, nouns were read at the same rate as the Repeat task, but subjects were asked to respond with a related verb (e.g., experimenter read "volcano," subject responded "erupt"). Additional control tasks used in some subjects were *Listen*, in which subjects were read common nouns and listened passively; *Nonwords*, in which subjects were read letters (e.g., "z") and listened passively; and *Covert generate*, in which subjects

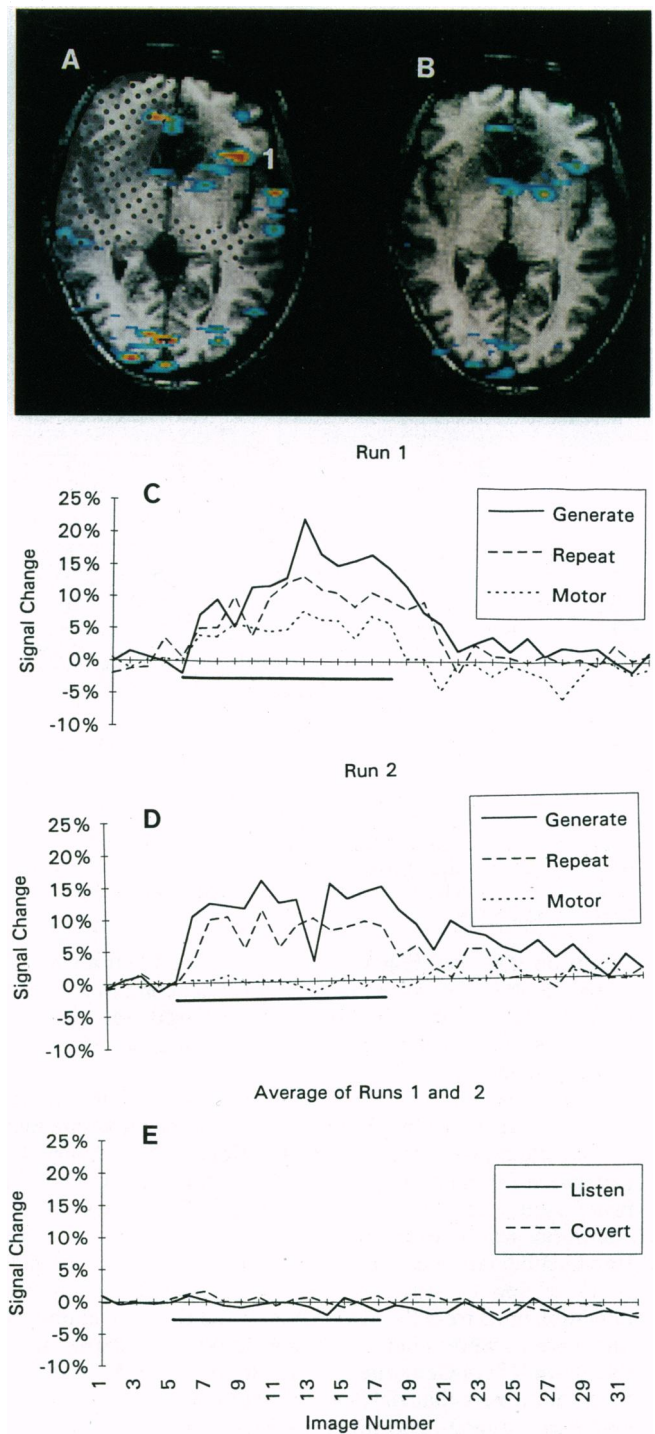


FIG. 2. (A) The color overlays represent z-score deviations of the first Generate condition from the first Baseline condition. ROI 1 includes infolded cortex and the anterior insula. (B) The color overlays represent a direct comparison of the Generate and Repeat conditions. (C and D) Time course of the activation effect for Generate, Repeat, and Motor measured for ROI 1 of A for the first and second replication of each condition, respectively. (E) Time course of the activation effect for the average of two replications of Listen and Covert measured for ROI 1 of A.

were asked to generate verbs mentally to the presented nouns but not to respond vocally.

**Data Analysis.** MRI data were processed as described (10). To isolate task-related intensity changes ( $\Delta S$ ) the static baseline was removed by subtracting voxel by voxel the mean of the five pre-task image ( $S_0$ ) from all 32 images in each



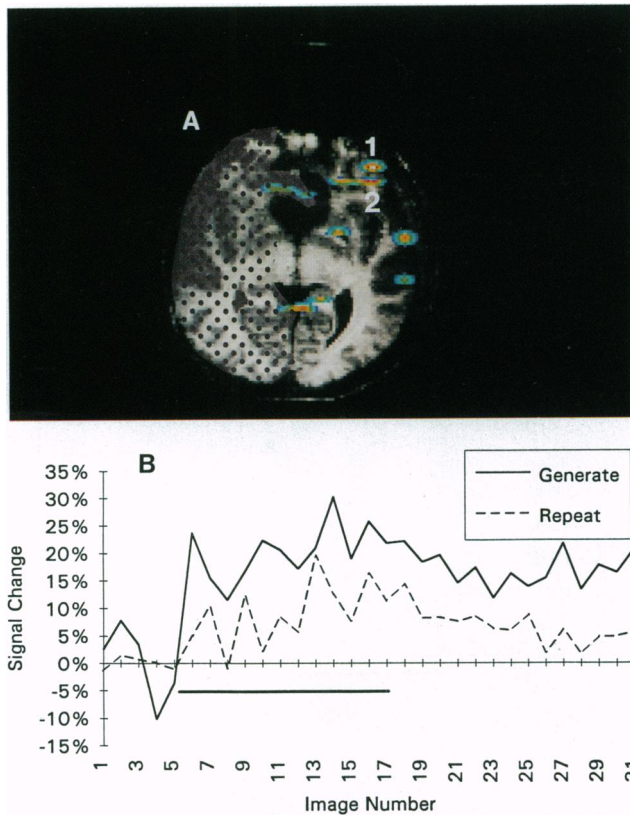


FIG. 3. (A) The color overlays represent z-score deviations of the first Generate condition from the first Baseline condition. (B) Time course of the activation effect for Generate and Repeat combined for ROIs 1 and 2 of A.

condition. The resulting  $\Delta S$  distribution was determined to be approximately Gaussian in the Baseline condition, which justified the use of normal-distribution-based statistics. The fractional signal change ( $\Delta S/S_0$ ) was computed for each voxel in each image.

A five-step automated procedure was used to identify voxels activated by the first replication of the Generate task. (i) The standard deviation of the fractional signal change was calculated for each voxel over the 32 images comprising the first Baseline condition. (ii) Each image of the first Generate condition was converted to z scores by dividing by the standard deviation calculated in step i. Thus, each voxel's z score during Generate expressed its change in standard deviation units from the same voxel in the Baseline condition. (iii) Voxels were selected during active task performance (images 6–17) of Generate whose z scores gave  $P \leq 0.05$ . (iv) Selected voxels that did not fall below half their activation levels in the post-task interval (18–32) were eliminated. (v) Finally, remaining voxels that were not adjacent to at least one other were eliminated. By enforcing a minimum particle size of two, we further decreased the likelihood that the activation pattern was due to random variation in signal intensity among voxels. This process was used to identify activated regions of interest (ROIs) in the first Generate condition that were used in all subsequent analyses. In the figures these ROIs, in z-score units, are overlaid upon  $T_1$ -weighted images of the selected plane.

Functional activity was measured in all conditions using these ROIs. The mean  $\Delta S/S_0$  for all voxels within each ROI was calculated for each of the 32 images for each condition and replication. Repeated-measures ANOVA was then performed to evaluate differences in functional activity for images 6–17 using task (Generate vs. Repeat vs. Motor) and replication as factors. When a significant main effect was

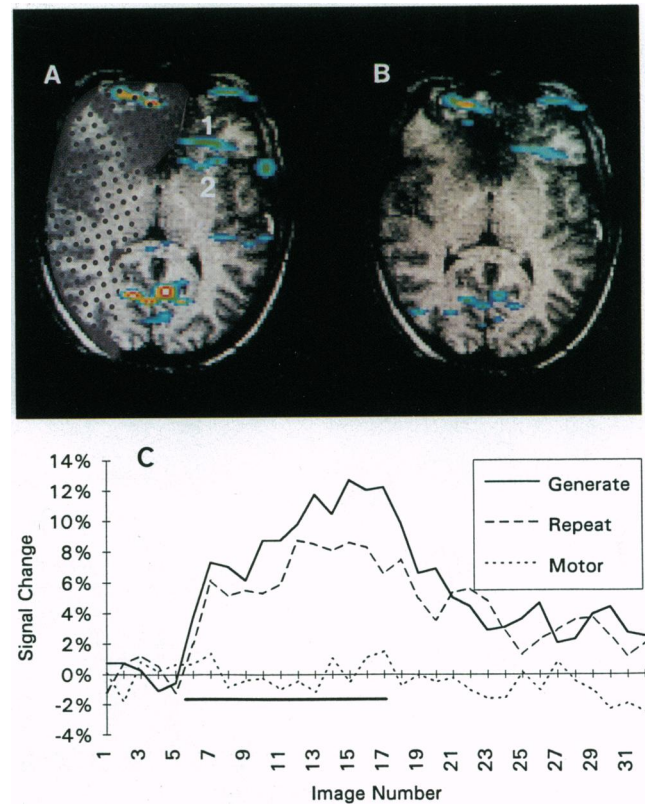


FIG. 4. (A) The color overlays represent z-score deviations of the first Generate condition from the first Baseline condition. (B) The color overlays represent a direct comparison of the Generate and Repeat conditions. (C) Time course of the activation effect for Generate, Repeat, and Motor measured for ROI 1 of A.

obtained, post-hoc pairwise comparisons of mean  $\Delta S/S_0$  were performed using Tukey's test with a criterion of  $P < 0.05$ .

In addition to these analyses based upon ROIs, *t* tests were computed on a voxel-by-voxel basis comparing image intensity during Generate and Repeat (images 6–17). These indicate regions that significantly differed in their activation between these two tasks.

## RESULTS

**Left Inferior Frontal Studies.** Fig. 1A shows the ROIs calculated by comparing the first Baseline and Generate conditions for subject one. A large ROI (marked as 1) is seen with two intense foci encompassing Brodmann's area 47 and extending anteriorly into area 10. Fig. 1C shows the time course of  $\Delta S/S_0$  for the Generate, Repeat, and Motor conditions. The lines are the mean over three replications of Generate and Repeat and two of Motor averaged over all voxels within the ROI. The largest response was obtained in Generate; a smaller response with a similar time course was obtained in Repeat. No effect was observed in Motor. ANOVA revealed a significant task effect during images 6–17 ( $P < 0.0001$ ). Post-hoc comparisons indicated that all three conditions significantly differed from each other. The signal change declined in magnitude in the third replication of the Generate and Repeat (data not shown).

The *t*-test image comparing Repeat and Generate is shown in Fig. 1B. The regions where Generate is most differentiated from Repeat in this alternative evaluation correspond to ROI 1 of Fig. 1A. The more medial and posterior focus is situated in infolded gray matter anterior to the lateral sulcus and may include the anterior insula. The more anterior foci probably includes areas 47 and 10. The activated regions include primarily gray matter; however, as the echo planar image was

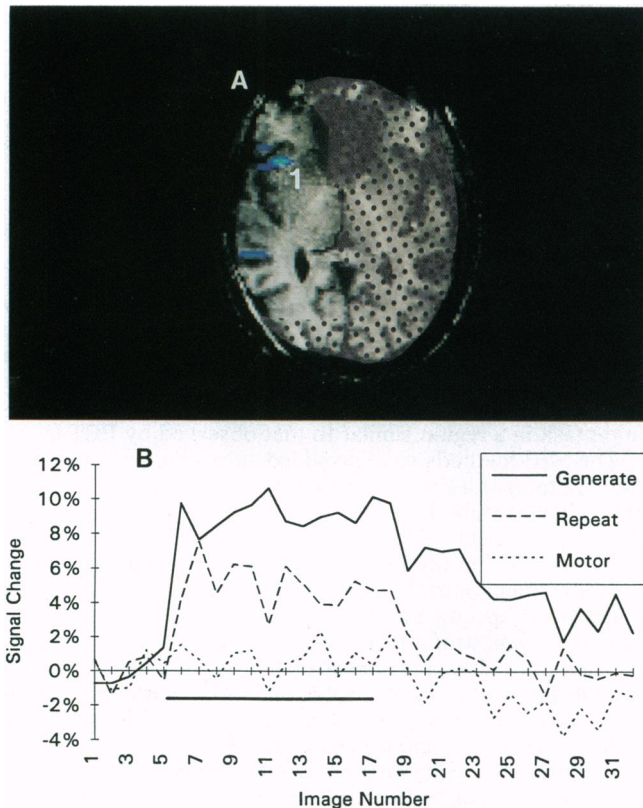


FIG. 5. (A) The color overlays represent z-score deviations of the first Generate condition from the first Baseline condition. In this image, shimming was optimized for the right inferior frontal cortex. These data were acquired on a separate day from the same subject whose LIFC data are shown in Fig. 2. The same color scale is used as in Fig. 2. (B) Time course of the activation effect for Generate, Repeat, and Motor measured for ROI 1 of A.

10 mm thick, an exact representation of the activation is limited by partial volume effects.

Fig. 2A presents the ROIs calculated comparing the first Baseline and Generate conditions for subject two. As before, a ROI (marked 1) encompasses the infolded gray matter anterior to the lateral sulcus in LIFC in Fig. 2A, and this same region is significant in the *t*-test image (Fig. 2B). Fig. 2C–E depict the activation time course for this ROI for the first (Fig. 2C) and second (Fig. 2D) replications of the Generate, Repeat, and Motor tasks. The time course was similar to that obtained from subject one. As before, ANOVA indicated that there was a significant effect ( $P < 0.0001$ ) and post-hoc Tukey tests indicated that all three conditions significantly differed in the activation period. The mean  $\Delta S/S_0$  for images 6–17 for Generate was 13% for run 1 and 12% for run 2, whereas for Repeat these values were 9% and 8%, respectively.

Fig. 2E presents the  $\Delta S/S_0$  time course obtained for ROI 1 of Fig. 2A for the Listen and Covert conditions. In this figure, the lines represent the mean of two replications. It is clear that neither task activated this region above pre-task levels.

Fig. 3A presents the ROIs calculated comparing the first Baseline and Generate conditions for subject three. ROIs 1 and 2 correspond anatomically to those seen in the previous two subjects. As ROI 1 and 2 showed similar activation patterns, their time courses have been combined in Fig. 3B. Generate and Repeat significantly differed ( $P < 0.002$ ). No significant activation was observed at these ROIs for the Listen and Nonwords conditions. The motor control condition was not performed.

Fig. 4A presents the ROIs calculated comparing the first Baseline and Generate conditions for subject four. ROIs 1

and 2 encompass two infolded regions of gray matter extending anteriorly (ROI 1) and medially (ROI 2) from the lateral sulcus. Both ROIs showed significant effects of task ( $P < 0.0001$ ), with Generate showing a significantly larger activation than Repeat, and with no observable activation for Motor. This can be seen in Fig. 4B, which shows the time course of activation for ROI 1.

Activation effects with similar time courses were observed in similar LIFC regions for the remaining three subjects. Subject 5 showed a similar activation pattern to the preceding subjects with a significant difference between Generate, Repeat, and Motor ( $P < 0.0001$ ). In subject 6 no activation was observed for Motor; however, Generate and Repeat showed the same level of activation ( $P < 0.0001$ ). In subject 7, Generate produced a significantly greater activation than Repeat ( $P < 0.006$ ); however, Motor produced significant activation that was intermediate in magnitude between Generate and Repeat. We did not observe activation in areas 10 and 47 for any subject in the Listen, Nonword, and Covert conditions.

**Activation Onset.** The mean  $\Delta S/S_0$  across images 6–17 for Generate across all subjects and replications was 10.5% for ROIs within the LIFC. To determine the onset of the activation effect in Generate, the mean  $\Delta S/S_0$  for image 5 (obtained just prior to task onset) was compared to images 6 and 7 (obtained, respectively, 3 and 6 s after task onset). Only the ROIs in LIFC were analyzed. The mean  $\Delta S/S_0$  for images 5–7 were 0.27%, 5.00%, and 9.24%, respectively. The signal change between images 5 and 6 was significant ( $P < 0.0007$ ), indicating that the task-related increase in signal exceeded the background level 3 s after task onset. The increase between images 6 and 7 was also significant ( $P < 0.018$ ).

**Right Hemisphere Studies.** In additional sessions the homologous right hemisphere regions of subjects 1 and 2 were optimally shimmed. In both cases an effect was noted. Activation during Generate was again larger than Repeat, and no activation was observed for Motor. Fig. 5A shows the results for subject 2, where ROIs 1 and 2 can be seen to encompass the same infolded cortical regional anterior to the lateral sulcus as for this subject's left hemisphere data (Fig. 2A). The time course of activation for these ROIs is presented in Fig. 5B and C, respectively.

**Validation of Results.** Two possible sources of artifactual signal change were examined. First, motion of the subject will produce voxel misalignment in difference images that could result in spurious signal changes within the ROI. This would be particularly problematic in ROIs that border cerebrospinal fluid (CSF). Second, generalized arousal causing increased blood flow to the entire cortex might cause signal intensity changes during the tasks. To assess these potential artifacts, three additional controls were carried out:

(i) In two subjects an adiabatic inversion pulse was added before the EPI sequence to null the CSF signal (15). CSF suppression during the Generate condition did not change  $\Delta S/S_0$ , indicating CSF contamination was not significant.

(ii) Functional imaging relies on the  $T_2^*$  weighting of the imaging sequence during which the signal evolves in the presence of local field gradients around the capillaries (6). Spin-echo images are insensitive to changes in local field gradients. Images were acquired with and without  $T_2^*$  weighting in two subjects for direct comparison during Generate. Activation was not observed in either subject using the spin-echo sequence without  $T_2^*$  weighting, confirming that the effect depended on differences in the internal magnetic fields as expected from deoxy-hemoglobin (Hb) blood flow changes.

(iii) In most subjects, activated regions were observed outside of the LIFC. To determine whether the activation was global, three subjects were run in additional sessions in which visual cortex was shimmed. As expected, no regions of activation were found in calcarine cortex. Thus the activation effect observed in frontal cortex was not simply the



result of an increased global blood flow. These studies further exclude subject movement related to speech as an artifact, as this movement would be expected to affect all regions of cortex. Outside of LIFC the anatomy in the slice varies with subject and for this reason other active ROIs were not analyzed in this study.

## DISCUSSION

The present tasks were modeled closely upon prior PET studies (1–3) that used the  $^{15}\text{O}$ -labeled water technique. We focused single slices upon the LIFC, which had been shown to be activated when subjects generated verbs from a noun. In agreement with PET, our results also show increased activity in this region during Generate compared to Baseline. The activation was statistically reliable in individual subjects and could be observed in single images obtained in 65 ms. This contrasts with PET studies, which usually require intersubject averaging.

The most consistent locus of the activation was Brodmann's area 47, near the Talairach coordinates reported by Petersen *et al.* (2). An infolded region of cortex running anterior to the lateral sulcus that appeared to include the anterior insula was particularly involved. Some involvement of area 10 was also seen. The ROIs identified in the present study are similar to the PET observations. Superimposition of our activated ROIs upon  $T_1$ -weighted anatomical images shows that the activation effect is located in gray matter.

Although the present results support the PET studies, there were two main differences. (i) Whereas the activation for Generate was greater than for Repeat, there was still significant activation for Repeat in this region that had not been previously reported in the PET studies. (ii) In the two subjects tested, we observed a similar pattern of activation in homologous regions of the right inferior frontal cortex. Although some right hemisphere activation has been observed in language tasks in the PET literature, activation of the right inferior frontal region for verb generation has not been previously reported.

Brain activation within this region during the tasks used here may be attributed to (i) semantic factors related to word processing and association and/or (ii) response factors that might be independent of the task performed. The consistently greater activation effect for Generate suggests that additional activity correlated with word association and/or semantic processing activates this region. However, the lack of activation for Covert generate or Listen suggests that speech (or response) production was necessary for activation in the present study. It is unlikely that the activation response is purely motor activity since, with one exception, mouth, tongue, and jaw movements did not activate this frontal region. Generate and Repeat differ in difficulty and in the cues provided for the response. Frith *et al.* (4) have previously emphasized that responding without external cues may be a crucial factor in activating this region. Response factors (in contrast to semantic factors) are more easily reconciled with the observation that similar activation effects were obtained in the right hemisphere. Additional tasks will be required to distinguish the relative contributions of response and semantic factors.

In the present study data acquisition was limited to one slice with  $6 \times 4.5$  mm in-plane resolution. Three-dimensional multislice data acquisition is currently possible with some reduction in temporal resolution but was not performed due to data storage limitations. With stronger gradients the sensitivity of the measurements would allow spatial resolution of

$3 \times 2$  mm in plane with greater improvements possible at higher magnetic fields or with longer image acquisition times.

The overall 10.5% signal change and 3- to 6-s activation onset are similar to the values noted during visual stimulation in our previous study (10). We noted considerable variability across subjects in the magnitude of the signal change that is probably due to partial volume effects and the criteria for defining the activated ROI.

## CONCLUSION

MRI with  $T_2^*$  weighted contrast, as originally proposed by Ogawa *et al.* (6) and applied by several groups to measure brain activation during sensory stimulation, has been used in this study to follow LIFC brain activation during verbal task performance. Activation was observed during a verb generation task in a region similar to that observed by PET (1–3).

The MRI methods have provided substantially better spatial and temporal resolution than previous PET studies and have allowed statistically reliable responses to be obtained in individual subjects. The improved spatial resolution and the ability to overlay the functional image precisely on a high-resolution anatomical image allowed the response to be mapped to a specific sulcus in this region. The time course of activation was useful in eliminating non-task-related signal changes. The dynamic aspect of the signal changes can be used in future studies to resolve activation patterns in complex behavioral tasks into their components by isolating different psychological processes in time.

The present results demonstrate the value of fast MRI in the localization of brain activity during cognitive tasks. This technique will undoubtedly lead to new insights in the cognitive and clinical neurosciences.

This work was supported by National Institutes of Health Grant DK-34576, National Institute of Mental Health Grant MH-05286, and the Department of Veterans Affairs.

- Petersen, S. E., Fox, P. T., Posner, M. I., Mintun, M. & Raichle, M. E. (1988) *Nature (London)* **331**, 585–589.
- Petersen, S. E., Fox, P. T., Posner, M. I., Mintun, M. & Raichle, M. E. (1989) *J. Cog. Neurosci.* **1**(2), 153–170.
- Petersen, S. E., Fox, P. T., Snyder, A. Z. & Raichle, M. E. (1990) *Science* **249**, 1041–1044.
- Frith, C. D., Friston, K. J., Liddle, P. F. & Frackowiak, R. S. J. (1991) *Neuropsychologia* **29**, 1137–1148.
- Belliveau, J. W., Kennedy, D. N., McKinstry, R. C., Buchbinder, B. R., Weisskoff, R. M., Cohen, M. S., Vevea, J. M., Brady, T. J. & Rosen, B. R. (1991) *Science* **254**, 716–719.
- Ogawa, S., Lee, T. M., Nayak, A. S. & Glynn, P. (1990) *Magn. Reson. Med.* **14**, 68–78.
- Bandettini, P. A., Wong, E. C., Hinks, R. S., Tikofsky, R. S. & Hyde, J. S. (1992) *Magn. Reson. Med.* **25**, 390–397.
- Kwong, K. K., Belliveau, J. W., Chesler, D. A., Goldberg, I. A., Weisskoff, R. M., Poncelet, B. P., Kennedy, D. M., Hoppel, B. E., Cohen, M. S., Turner, R., Cheng, H. M., Brady, T. J. & Rosen, B. R. (1992) *Proc. Natl. Acad. Sci. USA* **89**, 5675–5679.
- Ogawa, S., Tank, D. W., Menon, R., Ellermann, J. M., Kim, S., Merkle, H. & Ugurbil, K. (1992) *Proc. Natl. Acad. Sci. USA* **89**, 5951–5955.
- Blamire, A. M., Ogawa, S., Ugurbil, K., Rothman, D., McCarthy, G., Ellermann, J. M., Hyder, F., Rattner, Z. & Shulman, R. G. (1992) *Proc. Natl. Acad. Sci. USA* **89**, 11069–11073.
- Frahm, J., Merboldt, K.-D. & Hancike, W. (1993) *Magn. Reson. Med.* **29**, 139–144.
- Mansfield, P. (1977) *J. Phys. C: Solid State Phys.* **10**, L55–L58.
- Hayes, C. E., Edelstein, W. A., Schenck, J. F., Mueller, O. M. & Eash, M. (1985) *J. Magn. Reson.* **32**, 622–628.
- Gruetter, R. & Boesch, C. (1992) *J. Magn. Reson.* **96**, 323–334.
- Patt, S. L. & Sykes, B. D. (1972) *J. Chem. Phys.* **56**(6), 3182–3184.